

# Nonlinear combining of multiple laser beams in Kerr medium

Pavel M. Lushnikov and Natalia Vladimirova

Department of Mathematics and Statistics, University of New Mexico, USA

[plushnik@math.unm.edu](mailto:plushnik@math.unm.edu)

**Abstract:** We consider combining of multiple laser beams into a single near diffraction-limited beam by beam self-focusing (collapse) in a Kerr medium. The beams with the total power above critical are combined in the near field and then propagated in the Kerr medium. Nonlinearity results in self-focusing event, combining multiple beams into nearly a diffraction-limited beam that carries the critical power. Beam quality of the combined beam is analyzed as a function of the number of combining beams and the level of random fluctuations of the combining beams phases.

© 2022 Optical Society of America

**OCIS codes:** (190.0190) Nonlinear optics; (260.5950) Self-focusing (190.4370); Nonlinear optics, fibers; (140.3510) Lasers, fiber.

---

## References and links

1. D. J. Richardson, J. Nilsson, and W. A. Clarkson, "High power fiber lasers: current status and future perspectives," *J. Opt. Soc. Am. B* **27**, B63–B92 (2010).
2. C. Jauregui, J. Limpert, and A. Tünnermann, "High-power fibre lasers," *Nature Photonics* **7**, 861 (2013).
3. V. Gapontsev, F. A. Fomin, and M. Abramov, "Diffraction limited ultra-high-power fibre lasers," (2010). Paper AWA1 in Proc. Adv. Solid-State Photon. OSA Topical Meeting.
4. <http://www.ipgphotonics.com>.
5. C. Jauregui, H.-J. Otto, N. Modsching, J. Limpert, and A. Tünnermann, "Recent progress in the understanding of mode instabilities," in "Proceedings of SPIE. Conference on Fiber Lasers XII - Technology, Systems, and Applications," , vol. 9344, L. Shaw and J. Ballato, eds. (2015), vol. 9344, p. 93440J.
6. T. Y. Fan, "Experimental observations of the threshold-like onset of mode instabilities in high power fibre amplifiers," *IEEE J. Sel. Topics in Quant. Elec.* **11**, 567–577 (2005).
7. S. M. Redmond, D. J. Ripin, C. X. Yu, S. J. Augst, T. Y. Fan, P. A. Thielen, J. E. Rothenberg, and G. D. Goodno, "Diffraction coherent combining of a 2.5 kw fiber laser array into a 1.9 kw gaussian beam," *Opt. Lett.* **37**, 2832–2834 (2012).
8. P. M. Lushnikov and N. Vladimirova, "Nonlinear combining of laser beams," *Optics Letters* **39**, 3429–3432 (2014).
9. O. V. Shtyrina, A. M. Rubenchik, M. P. Fedoruk, and S. K. Turitsyn, "Spatiotemporal optical bullets in two-dimensional fiber arrays and their stability," *Physical Review A* **91**, 033810 (2015).
10. L. Bergé, S. Skupin, R. Nuter, J. Kasparian, and J.-P. Wolf, "Ultrashort filaments of light in weakly ionized, optically transparent media," *Rep. Prog. Phys.* **70**, 16331713 (2007).
11. S. N. Vlasov, V. A. Petrishchev, and V. I. Talanov, "Averaged description of wave beams in linear and nonlinear media," *Izv. Vys. Uchebn. Zaved. Radiofizika* **14**, 1353 (1971).
12. V. E. Zakharov, "Collapse of langmuir waves," *Sov. Phys. JETP* **35**, 908 (1972).
13. C. Sulem and P. L. Sulem, *Nonlinear Schrödinger Equations: Self-Focusing and Wave Collapse* (World Scientific, New York, 1999).
14. P. M. Lushnikov, S. A. Dyachenko, and N. Vladimirova, "Beyond leading-order logarithmic scaling in the catastrophic self-focusing of a laser beam in Kerr media," *Phys. Rev. A* **88**, 013845 (2013).
15. P. M. Lushnikov and H. A. Rose, "Instability versus equilibrium propagation of laser beam in plasma," *Phys. Rev. Lett.* **92**, 255003 (2004).
16. P. M. Lushnikov and H. A. Rose, "How much laser power can propagate through fusion plasma?" *Plasma Physics and Controlled Fusion* **48**, 1501–1513 (2006).

17. P. M. Lushnikov and N. Vladimirova, “Non-gaussian statistics of multiple filamentation,” *Opt. Lett.* **35**, 1965–1967 (2010).
  18. Y. Chung and P. M. Lushnikov, “Strong collapse turbulence in quintic nonlinear schrödinger equation,” *Physical Review E* **84**, 036602 (2011).
  19. T. S. Ross, *Laser Beam Quality Metrics* (SPIE Press, 2013).
  20. A. V. Smith and B. T. Do, “Bulk and surface laser damage of silica by picosecond and nanosecond pulses at 1064 nm,” *Applied Optics* **47**, 4812–4832 (2008).
  21. J. W. Dawson, M. J. Messerly, R. J. Beach, Miroslav, Y. Shverdin, E. A. Stappaerts, A. K. Sridharan, P. H. Pax, J. E. Heebner, C. W. Siders, and C. Barty, “Analysis of the scalability of diffraction-limited fiber lasers and amplifiers to high average power,” *Optics Communications* **16**, 13240–13266 (2008).
- 

## 1. Introduction

A quick increase of the output power of fiber lasers in the last two and half decades [1, 2] resulted in reaching  $\sim 10\text{kW}$  in 2009 for the diffraction-limited beam [3]. Currently, 10-kW single mode and up to 100-kW multimode continuous-wave commercial fiber lasers are available [4], although the beam quality is not yet specified. The growth of output power since 2009 has been mostly stagnated because of the encountered mode instabilities [2, 5]. Further increase of the total power of the diffraction-limited beam is possible through the coherent beam combining [6, 1], where the phase of each laser beam is controlled, aiming to produce a combined beam with a coherent phase. Beam combining has been successfully demonstrated only for several beams. E.g., Ref. [7] has achieved combining of five 500W laser beams into a 1.9kW Gaussian beam with a good beam quality,  $M^2 = 1.1$ .

Nonlinearity is expected to be the key issue for further output power scaling of coherent beam combining [1]. In Ref. [8] we proposed that instead of trying to overcome this difficulty with nonlinearity, one can use nonlinearity to our advantage. We proposed to combine multiple laser beams with uncorrelated phases into a diffraction-limited beam using strong self-focusing in a nonlinear waveguide. Difficulty of that proposal is a significant variation of the distance to the collapse and sensitivity to phase distribution of the laser beams at the entrance to the waveguide. To mitigate this problem and to avoid catastrophic collapse, which could damage the waveguide, several approaches were proposed in Ref. [8]. Another option is to work with multi-core fiber [9], which reduces the efficiency of nonlinear combining.

In this paper we consider a different approach to nonlinear beams combining that uses a slab of Kerr media instead of a waveguide. We now require that the phases of input beams are close to each other. The number of laser beams can vary significantly, as long as the total power exceeds the critical power of self-focusing. (In our simulations we used 3, 7 and 127 beams, but their number is straightforward to increase.) Figure 1a shows a schematic of the nonlinear beam combining in a slab of Kerr medium.

The paper is organized as follows. In Section 2 simulation settings are discussed together with the basic facts about collapses. Section 3 considers the beam quality  $M^2$  of the combined beam and its sensitivity to the fluctuations of the phases of combining beams. In Section 4 the main results of the paper are discussed.

## 2. Basic equations and simulation parameters

We assume that the pulse duration is long enough to neglect time-dependent effects. (We estimate the range of allowed pulse durations below.) The propagation of a quasi-monochromatic beam with a single polarization through a Kerr media is given by the nonlinear Schrödinger equation (NLSE) (see e.g. [10]):

$$i\partial_z\psi + \frac{1}{2k}\nabla^2\psi + \frac{kn_2}{n_0}|\psi|^2\psi = 0, \quad (1)$$

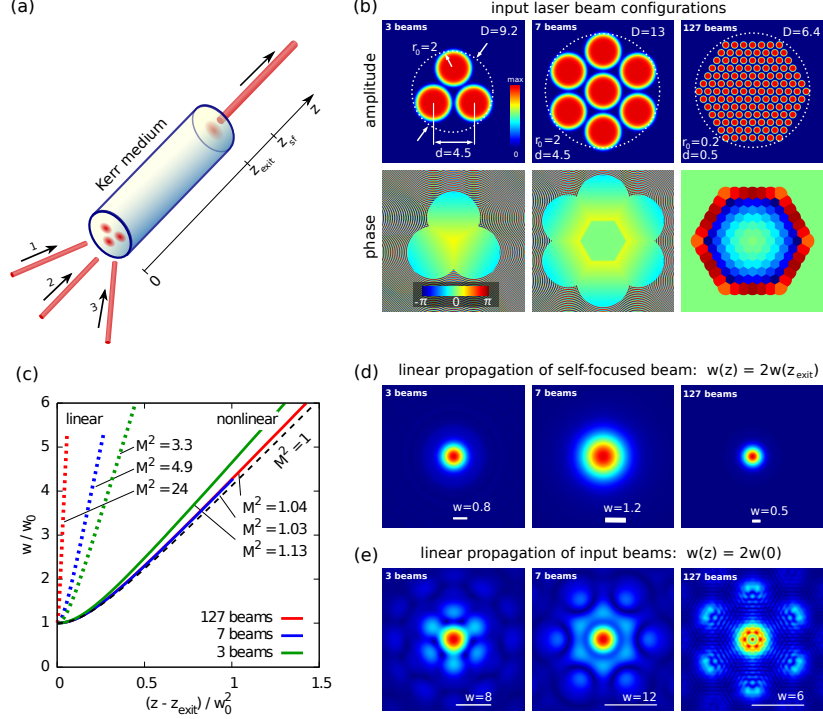


Fig. 1. (a) A schematic of 3-beam combining setup. (b) Amplitude and phase at the entrance surface for 3, 7 and 127 beams. (c)  $z$ -dependence of the beam width  $w$ . Solid lines are for propagation of self-focused beams in vacuum after exiting the Kerr medium at  $z = z_{\text{exit}}$ . Dotted lines of the same colors are for the propagation of input beams without Kerr medium ( $z_{\text{exit}} = 0$  in that case). A black dashed line is for propagation of Gaussian beam in vacuum with the beam quality factor  $M^2 = 1$ . (d) A cross-section of amplitude of the self-focused beam propagating in vacuum for  $z > z_{\text{exit}}$  (corresponds to solid lines in (c)) at the location where  $w(z) = 2w(z_{\text{exit}})$ . (e) A cross section of amplitude for beams propagating in vacuum (corresponds to solid lines in (c)) with  $z_{\text{exit}} = 0$  at the location where  $w(z) = 2w(0)$ .

where the beam is propagating along  $z$ -axis,  $\mathbf{r} \equiv (x, y)$  are the transverse coordinates,  $\psi(\mathbf{r}, z)$  is the envelope of the electric field,  $\nabla \equiv \left( \frac{\partial}{\partial x}, \frac{\partial}{\partial y} \right)$ ,  $k = 2\pi n_0/\lambda_0$  is the wavenumber in a medium,  $\lambda_0$  is the wavelength in the vacuum,  $n_0$  is the linear index of refraction, and  $n_2$  is the nonlinear Kerr index. The index of refraction is  $n = n_0 + n_2 I$ , where  $I = |\psi|^2$  is the light intensity. In fused silica  $n_0 = 1.4535$ ,  $n_2 = 3.2 \cdot 10^{-16} \text{cm}^2/\text{W}$  for  $\lambda_0 = 790 \text{nm}$  and  $n_0 = 1.4496$ ,  $n_2 = 2.46 \cdot 10^{-16} \text{cm}^2/\text{W}$  for  $\lambda_0 = 1070 \text{nm}$ . We bring NLSE (1) to the dimensionless form

$$i\partial_z \psi + \nabla^2 \psi + |\psi|^2 \psi = 0, \quad (2)$$

by the scaling transformation  $(x, y) \rightarrow (x, y)w_0$ ,  $z \rightarrow 2zkw_0^2$  and  $\psi \rightarrow \psi n_0^{1/2}/(2k^2 w_0^2 n_2)^{1/2}$ , where  $w_0$  is of the order of the waist of each input laser beam.

We also assume that the diameter of input beams in physical units is large enough for the applicability of NLSE (2) (it is sufficient for it to exceed several microns). All different cases of physical parameters considered below well satisfy this applicability condition.

NLSE (1) describes the catastrophic self-focusing (collapse) of the laser beam [11, 12],

provided the power  $P$  trapped in the collapse exceeds the critical value

$$P_c = \frac{N_c \lambda_0^2}{8\pi^2 n_2 n_0} \simeq \frac{11.70 \lambda_0^2}{8\pi^2 n_2 n_0}. \quad (3)$$

Here,  $N_c \equiv 2\pi \int R^2 r dr = 11.7008965 \dots$  is the critical power for NLSE (2) in dimensionless units and  $R(r)$ ,  $r \equiv |\mathbf{r}|$  is the radially symmetric Townes soliton [13]. The Townes soliton is defined as the ground state soliton of NLSE,  $\psi = e^{iz} R(r)$ , that is the solution of

$$-R + \nabla^2 R + R^3 = 0 \quad (4)$$

centered at  $\mathbf{r} = 0$ . In fused silica,  $P_c \simeq 2\text{MW}$  for  $\lambda_0 = 790\text{nm}$  and  $P_c \simeq 4.7\text{MW}$  for  $\lambda_0 = 1070\text{nm}$ . In air,  $P_c \simeq 2.4\text{GW}$  for  $\lambda_0 = 790\text{nm}$ .

Assume that  $N$  linearly polarized laser beams enter a Kerr medium at  $z = 0$ , as shown in Fig. 1. (We note that generalization to a case of arbitrary polarization is possible but is beyond the scope of this paper.) The initial condition for NLSE (2) is the superposition of the super-Gaussian beams,  $\psi(\mathbf{r}, z)|_{z=0} = \sum_{n=1}^N \psi_n$ , with  $\psi_n = A_n \exp\left(-\frac{(\mathbf{r}-\mathbf{r}_n)^8}{r_0^8} + i\phi_n\right)$ . Here  $r_0$ ,  $A_n$ ,  $\phi_n$  and  $\mathbf{r}_n$  are the width, the amplitude, the phase, and the location of the center of the  $n$ th beam, respectively. All beams have the same amplitude,  $A = A_n$ . In simulations with 3 or 7 beams, the beams of radius  $r_0 = 2$  are spaced at the distance  $d = 4.5$  between their centers, see Fig. 1b. In 127-beam simulation, the beams with  $r_0 = 0.2$  and spacing  $d = 0.5$  are packed in the hexagon pattern. The phases  $\phi_n$  vary between simulations. For simulations with 3 and 7 beams, we use  $\phi_n = \mathbf{k}_{n,\perp} \cdot (\mathbf{r} - \mathbf{r}_n)$ , where the transverse wavevectors  $\mathbf{k}_{n,\perp}$  have the same absolute value,  $\mathbf{k}_{n,\perp} = k_\perp$ , and are pointed to the origin so that  $\mathbf{k}_{n,\perp} = -k_\perp \mathbf{r}_n / |\mathbf{r}_n|$ . The only exception is the beam at the center for 7-beams case, where  $\mathbf{k}_{n,\perp} = \mathbf{0}$ . This phase distribution mimics the beams of constant phase entering the media at converging angles. In simulations with 127 beams, each beam has the plane wavefront with the constant phase  $\phi_n = -\frac{1}{2} \chi \mathbf{r}_n^2$ , so that the collection of all beams imitates the quadratic phase of a single pre-focused wide beam with the diameter  $D$  schematically shown by the dotted line in Fig. 1b.

To model nonlinear propagation, we use 4th order pseudospectral split-step method with adaptive resolution up to  $5120 \times 5120$  gridpoints in  $\mathbf{r}$  and adaptive stepping in  $z$ . Except for more sophisticated initial conditions, the major difference with earlier simulations [8] that we either did not use the waveguide or used waveguide (modeled by linear potential in the circular form) of the diameter above  $\gtrsim 3$  of the total initial diameter of all combined beams. Unless specified, the size of each simulation was chosen to be large enough to avoid influence of waveguide or domain boundaries on the resulting solutions.

Our choice of the combined power and distribution of all initial beams ensures strong self-focusing along  $z$  with the formation of the high amplitude beam (the collapsing filament) centered at  $\mathbf{r} = 0$ . The collapse is well approximated by the rescaled Townes soliton [13]:

$$|\psi(\mathbf{r}, z)| \simeq L(z)^{-1} R(\rho), \quad \rho \equiv r/L(z), \quad |\mathbf{r}| \equiv r, \quad (5)$$

where  $L(z)$  is the  $z$ -dependent beam width. The explicit form of  $L(z)$  dependence was found in Ref. [14], where it was confirmed that collapses with Gaussian initial conditions agree with  $L(z)$  starting from the amplitude  $|\psi|$  about 3-4 times above the initial value. In a similar way, the optical turbulence dominated by collapses [15, 16, 17, 18] results in well defined filaments of the form (5) as their amplitudes exceed the background values in 3-4 times. Combining of multiple beams, however, delays the formation of the solution (5) and typically requires 5-10 fold increase of initial amplitude to approach a diffraction-limited beam, as detailed Table 1.

### 3. Beam quality of the combined beam and effect of fluctuations of initial beam phases

We assume that after propagation through Kerr medium, the combined beam exits the medium at  $z = z_{\text{exit}}$  and propagates in vacuum for  $z > z_{\text{exit}}$ . Note that the beam exits nonlinear medium before it would reach nonlinear focus at  $z = z_{\text{sf}}$  if nonlinear medium were extended, i.e. we always choose  $z_{\text{exit}} < z_{\text{sf}}$ , as shown in Fig. 1a. We measure the beam quality factor  $M^2$  by fitting the effective width of the beam at  $z > z_{\text{exit}}$  with a quadratic function [19],

$$w^2(z) = w_0^2 + \left( \frac{2M^2}{k_0 w_0} \right)^2 (z - z_0)^2, \quad \text{where} \quad w(z) = \sqrt{2 \frac{\int |\psi|^2 r^2 d^2 \mathbf{r}}{\int |\psi|^2 d^2 \mathbf{r}}}. \quad (6)$$

Eq. (6) with  $M = 1$  is the exact solution for the propagation of a Gaussian beam in the vacuum. For non-Gaussian beams  $M^2 > 1$ . For general non-Gaussian beams the quantities  $w_0$ ,  $M^2$  and  $z_0$  are determined from the fit as follows. At the first step, we choose a range of  $z$  such that  $w^2(z)$  changes about twice compared with  $w_0^2$  to determine  $w_0$ ,  $M^2 = M_{\text{short}}^2$  and  $z_0$ . At the second step, we use a range of  $z$  where  $w^2(z)$  increases  $\sim 100$  times to fit for a new value of  $M^2 = M_{\text{long}}^2$ , with  $w_0$  and  $z_0$  obtained in the first fit. This scheme is different from proposed in [19] by using these two scales in  $z$ . Note that if a significant noise is present in the system, then the integration (6) can be done over areas where light intensity  $I = |\psi|^2$  exceeds a cutoff value,  $|\psi|^2 \geq I_{\text{cutoff}}$ , as suggested in Ref. [19]. However, we found that the cutoff introduces ambiguity in determining  $M^2$ , so we choose to integrate in (6) over the entire cross-section. To ensure good quality of the beam, we assumed that a diaphragm that removes all components with  $r > r_d = 3L(z_{\text{exit}})$  is installed at  $z = z_{\text{exit}}$ . Here,  $L(z)$  is determined by the rescaled Townes soliton (4), (5) as  $L(z) = R(0)/|\psi(\mathbf{0}, z)|$ , where  $R(0) = 2.20620 \dots$  [14]. Note that the diaphragm also removes the oscillating tails of Townes soliton [14], so the power of the filtered exit beam,  $P_d$ , is lower than the input power  $P$  and can fall below  $P_c$ .

Typical dependence  $w(z)$  in vacuum, obtained using Eq. (6), is shown in Fig 1c with  $M^2 \equiv M_{\text{long}}^2$  and  $P = 2P_c$ . The results of our simulations, summarized in Table 1, demonstrate very good quality of the combined beams, while propagation of the same input beams without self-focusing results in very low beam quality as shown in Fig. 1c. For a given input power, the increase of the pre-focusing parameter  $\chi$  allows to significantly reduce  $z_{\text{exit}}$  while keeping very good values of  $M^2$ , although sometimes at the expense of reducing  $P_d$ . The input power can be reduced even further (as least to  $1.6P_c$ ) if a Kerr waveguide is used instead of a slab of Kerr medium.

Last two columns of Table 1 provide physical values for the Kerr medium thickness,  $\tilde{z}_{\text{exit}}$ , and the input diameter,  $\tilde{D}$ , of all combined beams, as shown in Fig. 1b. To find these values we use  $n_0 = 1.4496$ , and  $n_2 = 2.46 \cdot 10^{-16} \text{ cm}^2/\text{W}$  for fused silica at  $\lambda_0 = 1070 \text{ nm}$ , which corresponds to the wavelength of the commercially available 100kW continuous-wave (cw) fiber laser [4]. We have also assumed that the maximum of intensity at  $z = z_{\text{exit}}$  is  $I = I_{\text{thresh}} \simeq 5 \cdot 10^{11} \text{ W/cm}^2$ . The value for  $I_{\text{thresh}}$  is obtained in experimental measurements of the optical damage threshold in fused silica for 8ns pulses [20]. If shorter pulses are considered then the threshold is increased, e.g.  $I_{\text{thresh}} \sim 1.5 \cdot 10^{12} \text{ W/cm}^2$  for 14ps pulses [20], while cw operation requires  $I_{\text{thresh}} \sim 10^9 \text{ W/cm}^2$  [21]. To use these alternative values, one need to re-evaluate the last two columns of Table 1 according to scaling used in Eq. (2). Note that neglecting contribution from a group velocity dispersion in Eq. (2) is justified for pulse durations above  $\sim 1 \text{ ps}$  for  $z_{\text{exit}}$  not exceeding several meters, as estimated in Ref. [8]. Contributions of stimulated Brillouin scattering and stimulated Raman scattering are estimated in Ref. [8].

We also studied a sensitivity of  $M^2$  to 10% random fluctuations of input beams phases and found that  $M^2$  changes by less than 1%, while the amplitude of the output beam is slightly reduced. Thus, the parameters of Table 1 ensure that no catastrophic collapse is possible for any random distribution of initial phases and optical damage of Kerr medium can be avoided.

	$k_{\perp}$ or $\chi$	$z_{\text{exit}}$	$ \psi_{\text{exit}} $	$ \psi_{\text{exit}}/\psi_0 $	$M_{\text{short}}^2$	$M_{\text{long}}^2$	$P_d/P_c$	$\tilde{z}_{\text{exit}}$ , cm	$\tilde{D}$ , mm
3 beams	0	4.10	4.90	5.43	1.189	1.183	1.0989	13.5	0.32
	0	4.25	9.98	11.07	1.119	1.119	1.0687	58.2	0.65
	0	4.29	20.43	22.66	1.114	1.114	1.0602	246.4	1.32
	0.3	2.00	5.31	5.89	1.201	1.194	1.1026	7.8	0.34
	0.3	2.10	9.12	10.11	1.134	1.134	1.0872	24.0	0.59
	0.3	2.14	17.07	18.94	1.131	1.131	1.0740	85.8	1.11
7 beams	0	7.65	5.12	8.68	1.156	1.155	1.0448	28	0.60
	0	7.82	9.85	16.69	1.109	1.109	1.0491	104	1.15
	0	7.86	17.81	30.19	1.107	1.107	1.0408	343	2.08
	0.3	5.15	5.02	8.51	1.034	1.034	1.0355	18	0.58
	0.3	5.29	10.05	17.04	1.090	1.090	1.0176	74	1.18
	0.3	5.34	18.77	31.82	1.090	1.090	1.0178	259	2.20
127 beams	0.5	0.373	6.95	5.01	2.065	1.858	0.9083	2.45	0.40
	0.5	0.435	11.17	8.05	1.038	1.037	0.9085	7.38	0.64
	1.0	0.196	6.94	5.00	1.941	1.796	0.9204	1.32	0.40
	1.0	0.220	11.15	8.04	1.592	1.572	0.8495	3.76	0.64
	1.0	0.231	13.75	9.91	1.141	1.135	0.8402	5.98	0.79
	2.0	0.106	6.93	5.00	1.526	1.516	0.6394	0.72	0.40
	2.0	0.115	11.02	7.94	1.417	1.412	0.6245	2.01	0.63
	2.0	0.122	13.85	9.98	1.363	1.359	0.6261	3.16	0.80

Table 1. Properties of self-focused beams formed by combining 3, 7, or 127 beams with total input power  $P = 2P_c$ : radial component of the wave vector,  $k_{\perp}$  (for the 3-beam and 7-beam cases) or phase shift parameter  $\chi$  (for the 127-beam case); maximum amplitude at the exit from nonlinear medium,  $|\psi_{\text{exit}}| \equiv |\psi(\mathbf{0}, z_{\text{exit}})|$ ; ratio of exit amplitude to input amplitude,  $|\psi_{\text{exit}}/\psi_0| \equiv |\psi_{\text{exit}}|/\max_{\mathbf{r}} |\psi(\mathbf{r}, 0)|$ ; quality of the exit beam filtered by the diaphragm of radius  $r_d = 3L(z_{\text{exit}})$ , measured at short distances  $M_{\text{short}}^2$  and at long distances  $M_{\text{long}}^2$ ; power of the exit beam filtered by the diaphragm,  $P_d$ ; thickness of the slab of the medium,  $\tilde{z}_{\text{exit}}$ , and total diameter of input beams,  $\tilde{D}$ , both in physical units. Here  $\tilde{z}_{\text{exit}} = (0.1376 \text{ cm}) z_{\text{exit}} |\psi_{\text{exit}}|^2$  and  $\tilde{D} = (0.0180 \text{ mm}) D |\psi_{\text{exit}}|$  for the intensity maximum  $I = 5 \cdot 10^{11} \text{ W/cm}^2$  at  $z = z_{\text{exit}}$ .

#### 4. Conclusion

In conclusion, we demonstrated the possibility of nonlinear beam combining by propagating multiple laser beams in a Kerr medium with realistic parameters. Table 1 shows that one can scale the medium thickness  $\tilde{z}_{\text{exit}}$  down to  $\sim 1 \text{ cm}$  and the medium width down to  $\sim 1 \text{ mm}$  in fused silica with  $\lambda_0 = 1070 \text{ nm}$ . Further improvements are possible if going beyond a flat distribution of amplitudes of input beams. Strong self-focusing forms a single beam of high quality with the power close to critical power of self-focusing. We demonstrated that random fluctuations 10% of the beams phases do not alter the obtained results. Note that if one allows the beams' phases to be completely random, then instead of a slab of Kerr medium a significantly longer waveguide is needed to achieve beam combining [8].

#### Acknowledgments

This work was supported by NSF grant No. DMS-1412140. Simulations were performed at the Center for Advanced Research Computing, UNM, and the Texas Advanced Computing Center using the Extreme Science and Engineering Discovery Environment, which was supported by NSF Grant No. ACI-1053575.